

# Radio-Loudness of Active Galactic Nuclei: Observational Facts and Theoretical Implications

Marek Sikora<sup>1,5\*</sup>, Łukasz Stawarz<sup>2,3,4</sup>, and Jean-Pierre Lasota<sup>5</sup>

<sup>1</sup>*Nicolaus Copernicus Astronomical Center, Bartycka 18, 00-716 Warsaw, Poland*

<sup>2</sup>*Landessternwarte Heidelberg, Königstuhl, D-69117 Heidelberg, Germany*

<sup>3</sup>*Max-Planck-Institut für Kernphysik, Saupfercheckweg 1, 69117 Heidelberg, Germany*

<sup>4</sup>*Astronomical Observatory, Jagiellonian University, ul. Orła 171, 30-244 Kraków, Poland*

<sup>5</sup>*Institut d'Astrophysique de Paris, UMR 7095 CNRS, Université Pierre et Marie Curie, 98bis Bd Arago, 75014 Paris, France*

Accepted .... Received ...; in original form ...

## ABSTRACT

We investigate how the radio-loudness of Active Galactic Nuclei (AGN) depends on their bolometric luminosity expressed in Eddington units (Eddington ratio) and on the central black-hole mass. In our sample we include the, often missed in other similar studies, broad-line-radio-galaxies (BLRG) and find that for the same range of Eddington ratios, the radio-loudness of BLRG is on average 3 orders larger than the radio-loudness of Seyfert galaxies. Both sub-samples form sequences along which the radio-loudness decreases with increasing Eddington ratio with slopes corresponding roughly to constant radio luminosity. At very low luminosities these two AGN sequences match respectively the sequences of FRI radio-galaxies and LINERS, but with an indication of a radio-loudness saturation. We show that these features can be naturally reproduced by assuming that the normalization of the dependence of radio-loudness on the Eddington ratio is determined by the black-hole spin and that central black holes in giant elliptical galaxies have on average spins much larger than black holes in the centers of spiral/disc galaxies. Finally, we address the issue of radio-loudness dichotomy among the near-Eddington AGN, and suggest that at high accretion rates jet production, and therefore radio-loudness, might be suppressed as is directly observed in several X-ray binaries.

**Key words:** galaxies: jets – radiation mechanisms: non-thermal – MHD

\* E-mail: sikora@camk.edu.pl

## 1 INTRODUCTION

It took several years from the discovery of first quasars to realize that most of them are radio-quiet rather than radio-loud. Strittmatter et al. (1980) pointed out that radio-loudness of quasars, defined as the radio-to-optical flux density ratio, may have a bimodal distribution. Radio bimodality was confirmed by Kellermann et al. (1989), who demonstrated that there are at least 5 – 10 times more radio-quiet than radio-loud quasars (see also Miller, Peacock, & Mead 1990; Stocke et al. 1992). However, most recent studies based on deep radio surveys FIRST and NVSS (Becker, White, & Helfand 1995; Condon et al. 1998), and optical massive surveys SDSS and 2dF (York et al. 2000; Croom et al. 2001), suggest that bimodality is rather weak, or even may not exist (White et al. 2000; Ivezić et al. 2002; Cirasuolo et al. 2003a,b).

The issue of radio-loudness recently got a new dimension: after astronomers had learned how to ‘weight’ supermassive black holes (see Woo & Urry 2002 and refs. therein), it became possible to study the dependence of the radio-loudness parameter,  $\mathcal{R} \equiv L_{\nu_R}/L_{\nu_{opt}}$ , on the Eddington ratio,  $\lambda \equiv L_{bol}/L_{Edd}$ . Here  $L_{\nu_R}$  and  $L_{\nu_{opt}}$  stand for the monochromatic luminosities at some specified radio,  $\nu_R$ , and optical,  $\nu_{opt}$ , frequencies, while  $L_{bol}$  and  $L_{Edd}$  denote bolometric luminosity of the active nucleus and the appropriate Eddington luminosity, respectively. The analysis of radio-loudness for PG quasars, Seyfert galaxies, and LINERS, performed by Ho (2002) seem to indicate that radio-loudness increases with decreasing Eddington ratio, however, with a huge scatter in  $\mathcal{R}$ . His results showed also that the largest  $\mathcal{R}$  are found in AGNs with black hole masses  $\geq 10^8 M_\odot$ . Such a mass-related duality was recently confirmed by Chiaberge, Capetti, & Macchetto (2005) who included in their sample FR I radio-galaxies. The effect, however, could not be clearly identified for intermediate Eddington ratios. We will show that the reason is that the above studies did not include broad-line radio galaxies (hereafter BLRGs). These objects are almost exclusively hosted by giant elliptical galaxies and, as it will be demonstrated in this paper, they cover a similar range of  $\lambda$  as Seyfert galaxies, but are about  $10^3$  times radio louder. The criteria for selection of BLRGs used in our studies are specified in §2. These sources are studied together with Seyfert galaxies, radio-quiet LINERS, FR I radio galaxies, and quasars. The results are presented in §3.

The studies of radio-loudness are crucial for addressing such basic questions as how jets are formed, accelerated and collimated, and why efficiency of the jet production can be so different even among objects looking very similar in all other aspects. The same questions concern jets in black-hole and neutron-star X-ray binaries (XRBs; see review by Fender 2004). Taking advantage of the very short time-scales of XRB variabilities, the dependence of the radio-loudness on the

Eddington ratio in these objects can be traced directly, for each source individually. Such studies indicate that at low luminosities the radio-loudness is a monotonic function of the accretion luminosity (Gallo, Fender & Pooley 2003), while at the highest luminosities it may jump by a large factor, following transitions between two accretion states (Fender, Belloni, & Gallo 2004). If the radio activity of individual AGNs depends on the Eddington ratio in a similar way, then the observed huge differences of radio-loudness for AGNs with similar Eddington ratio, especially at its lowest values, indicates that yet another parameter in addition to the accretion rate must play a role in determining the jet production efficiency. In §4 we investigate the possibility that the scatter of radio-loudness parameter can be related to a spin of a black hole. Our main results and their theoretical implications are concluded in §5.

In this paper we assume  $\Lambda$ CDM cosmology, with  $\Omega_M = 0.3$ ,  $\Omega_\Lambda = 0.7$ , and the Hubble constant  $H_0 = 70 \text{ km s}^{-1} \text{ Mpc}^{-1}$ .

## 2 SAMPLES

Our studies include: radio-loud broad-line AGNs (BLRGs plus radio-loud quasars); Seyfert galaxies and LINERS; FR I radio galaxies; optically selected quasars. The subsamples were selected to share the following criteria:

- the optical flux of the central, unresolved source is known;
- the total radio flux is known (including extended emission if present);
- black hole masses or necessary parameters to estimate them are available in literature.

Other criteria, applied individually to different subsamples, are specified below. In our sample, we did not include blazars, i.e., OVV-quasars, HP-quasars, and BL Lac objects, because their observed emission is significantly Doppler boosted. Here we also did not analyze narrow line radio galaxies (NRLGs), because their optical nuclei are hidden by “dusty tori”, which makes estimation of the accretion rates very uncertain.

### 2.1 Radio-selected broad line AGN

The objects are taken from Eracleous & Halpern (1994; 2003; hereafter EH94 and EH03, respectively) who studied profiles of the broad  $H\alpha$  emission lines of radio-loud AGNs with  $z \leq 0.4$ , selected from Véron-Cetti & Véron (1989). We divided the sample in two sub-groups: the radio-loud quasars and BLRGs, with the commonly used division line at  $M_V = -23$  which corresponds to the  $V$ -band luminosity  $L_V \simeq 10^{44.6} \text{ ergs s}^{-1}$ . They are listed in Tables A1 and A2, along with the

following data: IAU coordinates for the J2000.0 epoch; name of the source; redshift,  $z$ , with the most accurate values taken from EH04;  $V$ -band total apparent magnitude,  $m_V$ , taken from EH94 and EH03; Galactic extinction,  $A_V$ , available in NED (<http://nedwww.ipac.caltech.edu/>); starlight contamination,  $\kappa_*$ , taken from EH94 and EH03; total radio flux at  $\nu_5 \equiv 5$  GHz,  $F_5$ , obtained from the literature with references provided in the tables; FWHM of the  $H\alpha$  line taken from EH94 and EH04. We have used these data to calculate other quantities included in the tables, namely: the optical luminosity of the nucleus at  $\lambda_B \equiv 4400\text{\AA}$ ,  $L_B \equiv \nu_B L_{\nu_B}$ ; the radio luminosity at 5 GHz,  $L_R \equiv \nu_5 L_{\nu_5}$ ; the radio-loudness parameter,  $\mathcal{R} \equiv L_{\nu_5}/L_{\nu_B} = 1.36 \times 10^5 (L_R/L_B)$ ; the black hole mass,  $M_{\text{BH}}$ ; and finally the  $L_B$  and  $L_R$  luminosities expressed in the Eddington units.

The  $B$ -band nuclear luminosity was calculated using the standard luminosity-flux relation:

$$L_B = 4\pi d_L^2 \nu_B F_{\nu_B} (1+z)^{-(1-\alpha_{opt})}, \quad (1)$$

where  $d_L$  is the luminosity distance calculated for a given redshift and the assumed cosmology,  $\alpha_{opt}$  is the power-law slope around  $\nu_B$ , and the  $B$ -band nuclear flux is

$$\nu_B F_{\nu_B} = (\lambda_V/\lambda_B)^{(1-\alpha_{opt})} [-0.4(m_V - A_V) - 4.68] (1 - \kappa_*), \quad (2)$$

where  $\lambda_V \equiv 5500\text{\AA}$ , and  $\alpha_{opt} = 0.5$  is taken. In this paper we also assume the bolometric luminosity of the active nucleus  $L_{bol} = 10 L_B$ . The total radio luminosity of the source,  $L_R$ , was evaluated using analogous formula to the one given by Eq.(1), with the assumed radio spectral index  $\alpha_R = 0.8$  for the K-correction. We note, that most of the objects in this subsample are strong radio sources ( $F_5 > 0.03$  Jy), have radio-morphologies of the FR II type, and radio luminosities dominated by the extended structures. Radio fluxes for most of them were therefore taken from the single-dish radio surveys (Wright & Otrupcek 1990, Gregory & Condon 1991). In the case of three weak sources IRAS 02366-3101, MS 0450.3-1817, and CBS 74, for which the radio data from other facilities were used as indicated in the tables, the provided radio fluxes (and hence  $L_R$  and  $\mathcal{R}$  parameters) should be rather considered as lower limits. Finally, black hole masses for most of the Eracleous and Halpern objects are not available in literature. We estimated them using BLR size–luminosity relation assuming virial velocities of the gas which produces broad  $H\alpha$  lines (see, e.g., Woo & Urry 2002 and references therein),

$$\frac{M_{\text{BH}}}{M_\odot} = 4.8 \times \left[ \frac{\lambda L_\lambda(5100\text{\AA})}{10^{44}\text{ergs/s}} \right]^{0.7} \text{FWHM}_{H\alpha}^2, \quad (3)$$

where  $\text{FWHM}_{H\alpha}$  is derived by EH94 or EH03, and  $L_\lambda(5100\text{\AA}) = (\lambda_B/5100\text{\AA})^{(1-\alpha_{opt})} L_B$ .

## 2.2 Seyfert galaxies and LINERS

This sample contains objects selected from Ho & Peng (2001) and Ho (2002; hereafter HP01 and H02, respectively). All objects studied by HP01 have Seyfert 1 type nuclei and are taken from Palomar and CfA surveys. We have selected only those for which estimations of black hole masses were available in literature. The sample of H02 is composed by AGNs with given black hole masses and includes Seyfert galaxies, LINERS, Transients, and PG quasars. We included only AGNs for which at least the  $H\alpha$  line is broad, i.e., we did not include galaxies with nuclei of spectral type S2, L2, and T2. We did not include here PG quasars — they are treated by us separately (see §2.4). The final ‘Seyferts + LINERS’ sample is made from 39 objects (36 galaxies with Seyfert nuclei and 3 LINERS) listed in Table A3. The table encloses information about IAU coordinates for the J2000.0 epoch; name of the source; distance of the source,  $d$ ; absolute  $B$ -magnitude of the nucleus,  $M_B$ ;  $B$ -band luminosity of the nucleus,  $L_B$ ; total radio luminosity at 5 GHz,  $L_R$ ; radio-loudness parameter,  $\mathcal{R}$ ; black hole mass,  $\mathcal{M}_{\text{BH}}$ , followed by the appropriate reference; and finally the  $B$ -band and radio luminosities in the Eddington units.

Distances, if less than 40 Mpc ( $z < 0.009$ ), are the same as adopted by H02 from Tully (1988). They were derived taking into account the effect of the Virgo infall. If larger, the values given in H02 were multiplied by a factor ( $0.75/0.7$ ), due to the difference in the value of the Hubble constant used in H02 and in this paper. Absolute  $B$ -magnitudes of nuclei,  $M_B$ , were taken from HP01 if available. These are the values calculated from directly measured apparent magnitudes  $m_B$  of the nuclear regions. In other cases,  $M_B$  were taken from H02. These are obtained from the  $L_{H\beta} - M_B$  correlation. For distances to the source larger than 40 Mpc, the absolute magnitude  $|M_B|$  was increased by a factor ( $2.5 \log[0.75/0.7]^2$ ). The nuclear luminosity,  $L_B$ , was then calculated from the absolute  $B$ -magnitude,  $M_B$ , using the standard relation

$$\log L_B = 0.4 |M_B| + 35.6. \quad (4)$$

Regarding the radio emission, contrary to HP01 and H02, we decided to use in our studies of the AGN radio-loudness the total luminosities, i.e. including nuclear and extended emission (see §3.4). The total radio luminosities are taken from H02 and HP01 and as the optical luminosities they are corrected to account for different values of the Hubble constant.

## 2.3 FR I radio galaxies

Our sample of FRI radio galaxies consists of objects which were observed by Hubble Space Telescope and hence have determined optical luminosities (or the appropriate upper limits) for their

unresolved cores (see Kharb & Shastri 2004, and references therein) and in addition estimated black hole masses (Cao & Rawlings 2004; Woo & Urry 2002). Such sample contains 31 objects listed in Table A4 along with the optical and radio data: the IAU coordinates for the J2000.0 epoch; name; redshift,  $z$ ;  $B$ -band luminosity  $L_B$ , obtained after recalculating  $V$ -band luminosities provided by Kharb & Shastri (2004) to the cosmology we are using and then converted to  $B$ -band assuming optical spectral index  $\alpha_{opt} = 0.5$ ; total radio flux at 5 GHz,  $F_5$ , obtained from the literature indicated in the table (and if originally provided at other frequencies, recalculated assuming radio spectral index  $\alpha_R = 0.8$ ); total 5 GHz radio luminosity,  $L_R$ ; radio-loudness parameter,  $\mathcal{R}$  (assuming that the accretion luminosity is equal to the one observed from the optical core by HST); black hole mass,  $\mathcal{M}_{BH}$ , taken from Woo & Urry (2002) and Cao & Rawlings (2004); and finally  $B$ -band and radio luminosities expressed in the Eddington units.

## 2.4 PG quasars

This sample consists of those BQS objects (Schmidt & Green 1983) which have redshift less than  $z = 0.5$ , black hole mass available in literature, and are not included in our other sub-samples. The BQS objects are commonly called PG (Palomar-Green) quasars, despite the fact that not all of them satisfy the formal luminosity criterion  $M_V$  or  $M_B < -23$  to be classified as quasars (there are 7 of such BQS AGNs in our sample). The sample is listed in Table A5, along with the optical and radio data: the IAU coordinates for the J2000.0 epoch; name; redshift,  $z$ ;  $B$ -band luminosity  $L_B$ , calculated for  $m_B$  given by Schmidt & Green (1983);  $F_5$ , obtained from Kellerman et al. (1989); total 5 GHz radio luminosity,  $L_R$ ; radio-loudness parameter,  $\mathcal{R}$ ; black hole mass,  $\mathcal{M}_{BH}$ , taken from Vestergaard (2002) or Woo & Urry (2002); and finally  $B$ -band and radio luminosities expressed in the Eddington units.

## 3 RESULTS

### 3.1 Global patterns

Radio luminosities vs. optical luminosities of the selected AGNs are plotted in Figure 1. As can be seen our sub-samples form two sequences which are separated by  $\sim 3$  orders of magnitude in radio luminosity. One can check from the Tables A1-A5, that the upper sequence is almost exclusively populated by the objects with the black hole masses  $\mathcal{M}_{BH} > 10^8 \mathcal{M}_\odot$ . Among them there is only one object from the 'Seyferts plus LINERS' sub-sample, NGC 1275. It should be noted, however, that this object, as all the others in the upper sequence, is hosted by a giant elliptical

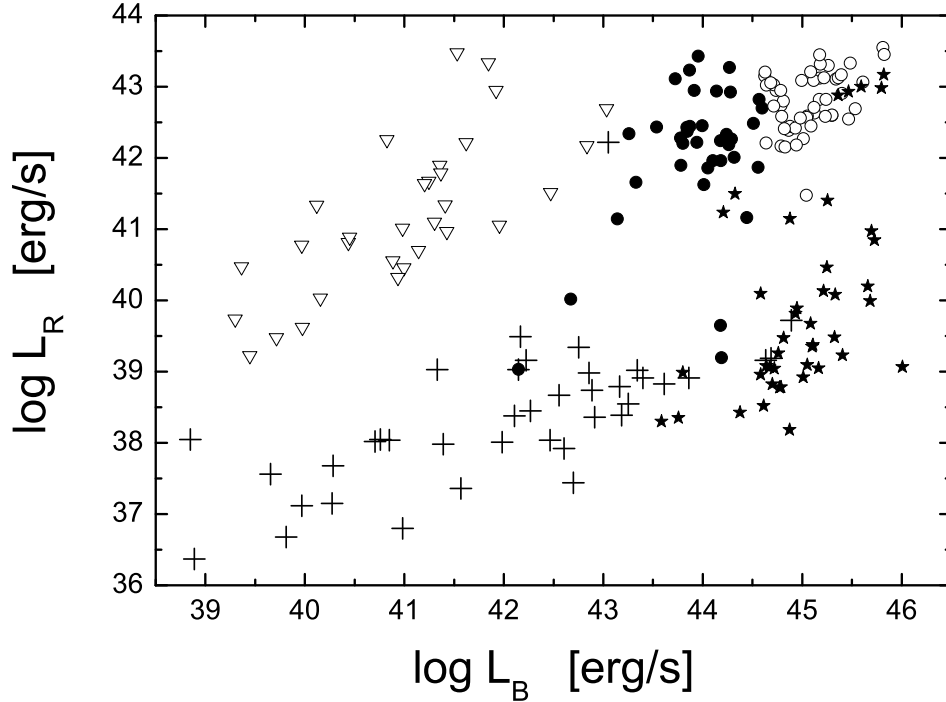


**Figure 1.** Total 5 GHz luminosity vs.  $B$ -band nuclear luminosity. BLRGs are marked by filled circles, radio-loud quasars by open circles, Seyfert galaxies and LINERS by crosses, FR I radio galaxies by open triangles, and PG Quasars by filled stars.

galaxy (specifically, by the cD galaxy of the Perseus cluster), and has an extended FR I-like radio structure observed presumably at a small angle to the line of sight (Pedlar et al. 1990). Close to the upper sequence but still belonging to the ‘Seyferts plus LINERS’ subsample is located NGC 4258 (M106). This spiral galaxy hosts an extremely weak AGN. Its total radio luminosity is about 100 times larger than the nuclear one, and most likely is not related to the jet activity.

Whereas there are no disc-galaxy-hosted AGNs in the upper sequence, AGNs hosted by giant elliptical galaxies are present in both upper and lower sequences. This particularly concerns highest accretion luminosity objects, i.e. quasars. Most of them in fact, even those with very massive black hole and resolved elliptical hosts, occupy the lower sequence which we will call hereafter the ‘radio-quiet sequence’ (see §4.1). At intermediate accretion luminosities, AGNs hosted by giant elliptical galaxies and located in the lower sequence are represented in our sample only by four objects. However, recent discoveries of many radio-quiet galaxies with very broad Balmer lines and hosting very massive black holes (Strateva et al. 2003; Wu & Liu 2004) strongly indicate that rareness of such objects in the Eracleous & Halpern samples might be due only to selection ef-

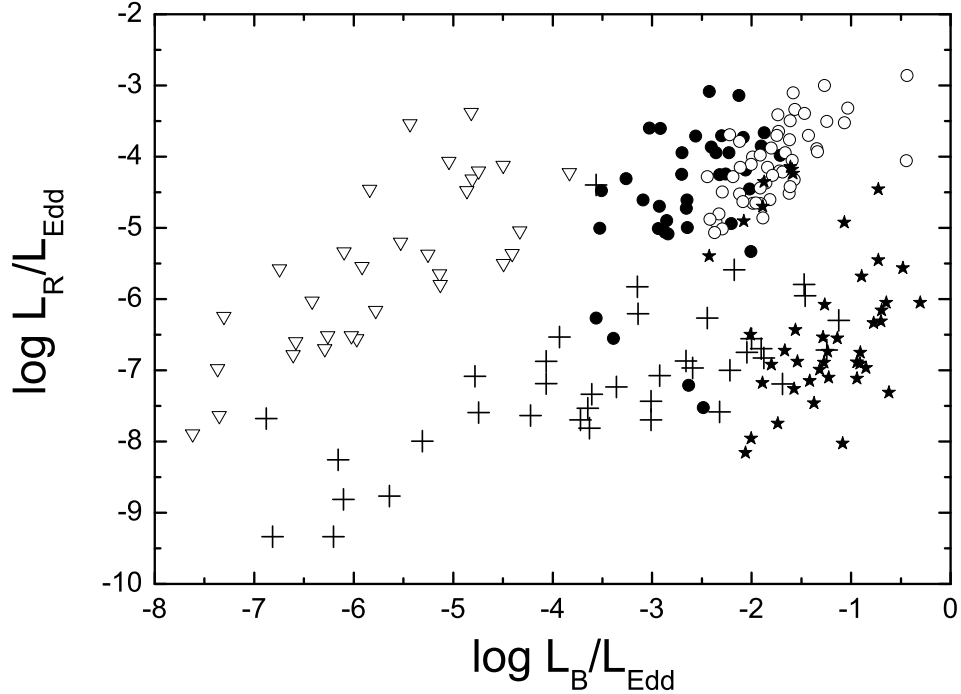


**Figure 2.** Total 5 GHz luminosity vs.  $B$ -band nuclear luminosity in the Eddington units. BLRGs are marked by the filled circles, radio-loud quasars by the open circles, Seyfert galaxies and LINERS by the crosses, FR I radio galaxies by the open triangles, and PG Quasars by the filled stars.

fects. Hence, it is plausible that also at intermediate accretion luminosities, most of AGNs hosted by giant elliptical galaxies are radio-quiet.

An intriguing feature of the Figure 1 is that both the radio-quiet sequence and the ‘radio-loud’ upper sequence have a similar dependence of radio-luminosity on the accretion-luminosity. It corresponds to an approximate constancy of  $L_R$  at larger values of  $L_B$  and to a decrease of  $L_R$  at smaller accretion rates. As shown in Figure 2, qualitatively the same feature is found when luminosities are expressed in Eddington units. The main difference between Figures 1 and 2 is the relative location of the two sequences which reflect the fact that AGN black-holes in the radio-loud sequence are on average  $\sim 20$  times more massive than black holes in AGNs forming the radio-quiet sequence. This causes a left-down shift of the upper sequence in Figure 2 relative to the lower sequence. Obviously due to a wide range of black hole masses in each of the sequences there are quantitative differences in the location of individual objects within the sub-samples. Furthermore, at the largest accretion luminosities, where the lower pattern is occupied mostly by the quasars hosted by giant elliptical galaxies, the relative location of the two sequence is not significantly modified.



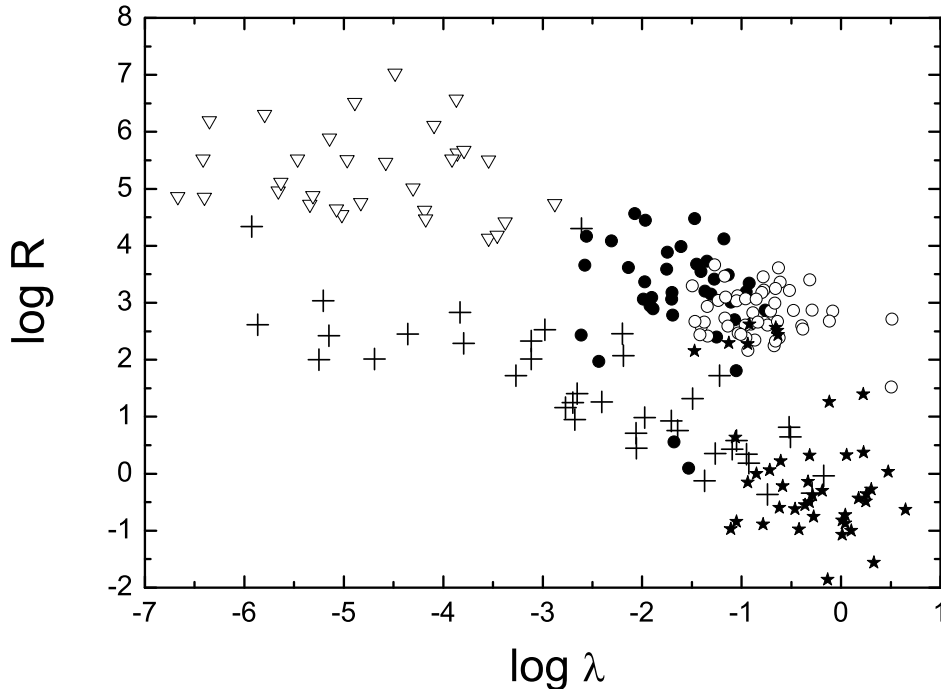


**Figure 3.** Radio-loudness  $\mathcal{R}$  vs. Eddington ratio  $\lambda$ . BLRGs are marked by the filled circles, radio-loud quasars by the open circles, Seyfert galaxies and LINERS by the crosses, FR I radio galaxies by the open triangles, and PG Quasars by the filled stars.

In Figure 3, we plot the dependence of the radio-loudness,  $\mathcal{R}$ , on the Eddington ratio,  $\lambda$ , assuming  $\lambda = L_{bol}/L_{Edd} = 10(L_B/L_{Edd})$  (see, e.g., Richards et al. 2006).<sup>1</sup> Our results confirm the trend of the increase in the radio-loudness with the decreasing Eddington ratio, originally noticed by Ho (2002; see also Merloni, Heinz, & Di Matteo 2003; Nagar, Falcke, & Wilson 2005). However, we show in addition that this trend is followed separately — with a large difference in normalization — by the ‘radio-quiet’ and the ‘radio-loud’ sequences. Yet another feature revealed in Figure 3 is a clear change of slope of the  $\mathcal{R} - \lambda$  dependence indicating some sort of saturation of radio-loudness at low Eddington ratios. A similar trend can be noticed, but specifically for FR I and FR II radio galaxies, in the data presented by Zirbel & Baum (1995). Let us recall that almost all BLRGs and radio-loud quasars in our samples have FR II radio morphology.

Finally, in Figure 4 we illustrate the dependence of radio-loudness on black-hole mass. This plot demonstrates that AGNs with the black hole masses  $> 10^8 \mathcal{M}_\odot$  reach values of radio-loudness

<sup>1</sup> Note that for very low luminosity AGNs the bolometric correction can be a factor  $\sim 2$  larger than considered above. However, due to very large uncertainties and not known functional dependence of the exact correction factor on the luminosity (Ho 1999), we decided to use the same proportionality constant for all the analyzed AGNs.

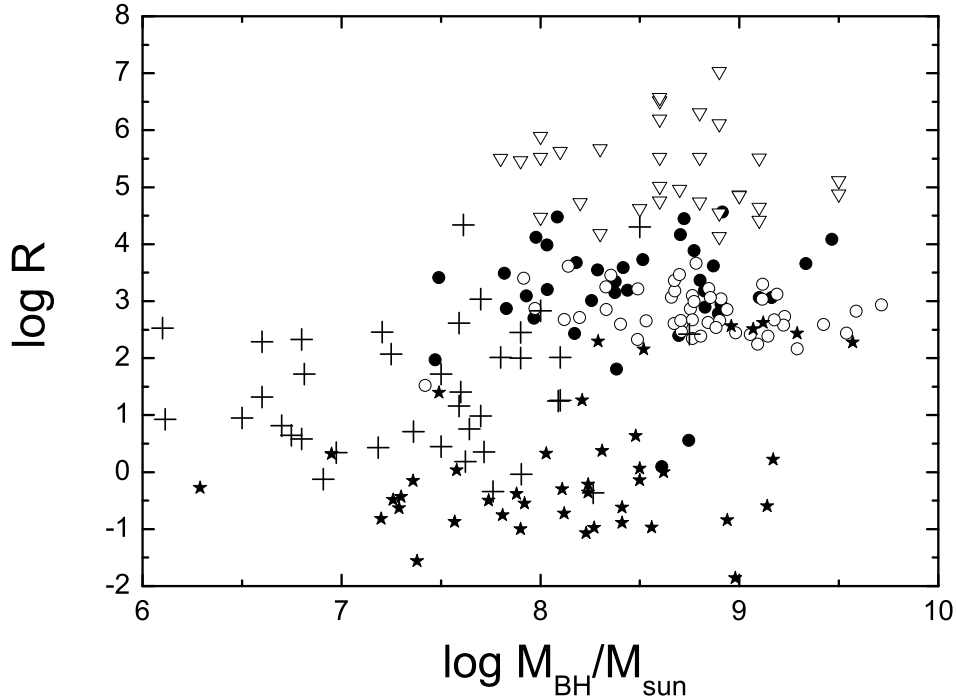


**Figure 4.** Radio-loudness vs. black hole mass. BLRGs are marked by the filled circles, radio-loud quasars by the open circles, Seyfert galaxies and LINERS by the crosses, FR I radio galaxies by the open triangles, and PG Quasars by the filled stars.

three orders of magnitude larger than AGNs with black hole masses  $< 3 \times 10^7 \mathcal{M}_\odot$ . A relatively smooth transition between those two populations most likely is caused by the overlap between black hole masses hosted by disc and elliptical galaxies. Errors in black hole mass estimations can also have a similar effect. It is interesting to compare our Figure 4 with the analogous figures restricted to high Eddington-ratio objects presented by Laor (2003) and McLure & Jarvis (2004). One can see that in all cases there is a difference of about 3 orders of magnitude between the maximal radio-loudness of AGNs with  $\mathcal{M}_{\text{BH}}/\mathcal{M}_\odot > 10^8$  and AGNs with less massive black holes. However, because in our sample we have included AGNs with very low Eddington-ratios the boundaries of maximal radio-loudness for less and more massive objects are now located at much larger  $\mathcal{R}$ . This effect is a simple consequence of the radio-loudness increasing with the decreasing Eddington-ratio. Because of this, the upper radio boundaries are determined by low- $\lambda$  objects: in the lower- $\mathcal{M}_{\text{BH}}$  sub-group by Seyferts and LINERS, in the larger- $\mathcal{M}_{\text{BH}}$  sub-group by FR I radio galaxies.

### 3.2 Incompleteness of our sample and related uncertainties

Our sample is very heterogeneous, being composed from incomplete sub-samples selected using different criteria. This must have effects on the presented plots and should be taken into account when interpreting our results. The largest incompleteness concerns the broad-line AGNs taken from the radio-selected samples. They include BLRGs and radio-loud quasars, which are all associated with giant elliptical galaxies. However, as known from radio studies of optically selected quasars, the majority of such sources are radio-quiet and many are radio-intermediate (White et al. 2000). The same was recently found for lower- $\lambda$  objects, when investigating the double-peaked broad emission lines in AGNs from the SDSS catalog (Strateva et al. 2003). Contrary to the deeply grounded conviction that the presence of double-peaked lines is unique to BLRGs, it was discovered that such lines are pretty common in radio-quiet AGNs with black hole masses characteristic of giant elliptical galaxies (Wu & Liu 2004). Noting all that, one should consider the upper, radio-loud sequence in our plots as populated only by a minority of the elliptical-hosted AGNs. In other words, with a complete (though not yet available) sample, the mid-Eddington AGNs in giant elliptical galaxies would not be confined to the upper sequence, but would show continuous distribution down to the lowest detectable radio levels, similarly to the PG quasars in our sample.

Meanwhile, the results presented by Wu & Liu (2004) in the right panels of their Figure 1 seem to indicate that for  $\lambda < 10^{-3}$  the proportions between radio-loud and radio-quiet fractions discussed above can reverse, i.e., that for  $\lambda < 10^{-3}$  the upper sequence is populated by the majority of the elliptical-hosted AGNs. This seems to be confirmed by relatively complete surveys of nearby galaxies, for which the prospect of missing radio-quiet AGNs among giant elliptical galaxies is rather low.

Finally, our sample is incomplete also because it does not include narrow-line Seyferts 1 (NLS1). These objects are presumably hosted by disc galaxies and represent high accretion-rate AGNs with relatively low black hole masses. They are radio-quiet as a class (Ulvestad, Antonucci, & Goodrich 1995), with only a few reaching  $\mathcal{R} > 100$ , and none producing a prominent extended radio structure (Zhou & Wang 2002; Whalen et al. 2006; Komossa et al. 2006). If included in our plots, they would form extension of the lower, radio-quiet pattern to large  $\lambda$ 's.

### 3.3 Potential errors and attempts to minimize them

Some quantities used to construct our plots can be subject to significant errors. This primarily concerns galaxies with very weak nuclei. Sometimes it is even difficult to decide whether the observed

nuclear features are dominated by the AGN or starburst activities, and thus what is the real accretion luminosity. To avoid the impact of such uncertainties on our results we did not include in the ‘Seyferts + LINERS’ sample objects of spectral type 2, i.e. those with no broad lines. On the other hand, uncertainties concern also sources with broad-line nuclei, firstly because of the accretion-luminosity contamination by starlight, and secondly because of the internal extinction. To avoid these uncertainties, Ho (2002) calculated accretion luminosities indirectly, using the correlation of the accretion luminosity (or more precisely – absolute magnitude  $M_B$ ) with the intensity of the  $H\beta$  line. However, as one can see in Ho & Peng (2001), this correlation is reasonable only for very luminous objects. Therefore, to minimize the related uncertainties, for sources overlapped by samples from Ho & Peng (2001) and Ho (2002), we adopted nuclear luminosities obtained in Ho & Peng from the direct optical measurements and corrected by subtracting the starlight.

Our selection of FR I radio-galaxies is less rigorous: in this subsample we have included also the objects for which there are no direct signatures of the accretion flow. We note that the correlation between the optical fluxes of the nuclear cores observed by HST in these sources and their radio fluxes suggests that the observed nuclear emission is due to synchrotron radiation originating in the inner portions of the jets (Verdoes Kleijn et al. 2002). Hence, in several papers it was assumed that HST detections provide the upper limits for the optical radiation due to the accretion flow (see, e.g., Chiaberge, Capetti, & Celotti 1999; Chiaberge, Capetti, & Macchetto 2005). However, it does not have to be the case if the central nuclei are hidden by “dusty tori”. Then the situation might be the opposite: the accretion luminosity can be in fact larger than the luminosity measured by HST. Arguments in favor of such a possibility are provided by Cao & Rawlings (2004), who postulated that indeed BL Lac objects accrete at the high rates. There are, however, strict limits on the bolometric luminosity of hidden AGN: it cannot be larger than the observed infrared luminosity resulting from reprocessing of the hidden nuclear radiation by the circumnuclear dust. Infrared observations clearly indicate that active cores in FR I’s radiate several orders of magnitude below the Eddington level (Knapp, Bies, & van Gorkom 1990; Müller et al. 2004; Haas et al. 2004). By comparing the infrared luminosities with the HST measurements for a number of FR I radio galaxies included in our sample, we find that the accretion luminosities of some of them might be underestimated by a factor larger than 10.

Other errors which may significantly affect details of our plots come from the estimations of black-hole masses. For all the objects except BLRGs and radio-loud quasars, these masses were taken from the literature. They were obtained using variety of methods. However, by comparing Figure 1 and 2, which are constructed with and without involving black hole masses, respectively,

one can see that such global features as two-sequence structure and the general trends survive. Hence we conclude that our results are not significantly affected by errors of black-hole mass estimations.

Finally, one should comment on our choice of calculating the radio-loudness parameter by using not the strictly nuclear radio fluxes (as in several other similar studies) but the total ones. In the cases of lobe-dominated radio quasars, BLRGs, and FR I radio galaxies, the observed radio luminosity is produced mainly by jet-powered extended radio structures. As long as our interest in radio-loudness is to understand the strong diversity of the jet power, the extended radio component should be therefore considered. Less obvious is the situation in the case of AGNs hosted by spiral galaxies. There the nuclear radio emission is usually dominant while the extended radio emission can be not only due to the jet activity, but also to the starburst regions. Hence by using total radio fluxes, as did in this paper, one can overestimate radio-loudness (which should concern only the jet-related emission). Such a choice is however more appropriate than taking into account only the nuclear radio component: in this way we avoid eventual underestimation of the radio-loudness, which would artificially increase the gap between the upper and lower patterns in Figures 1-3. In other words, with our choice is conservative.

## 4 DISCUSSION

### 4.1 Radio-loudness vs. galaxy morphology

Using several subsamples of AGNs which together cover seven decades in the Eddington ratio, we have demonstrated that radio-selected AGNs hosted by giant elliptical galaxies can be about  $10^3$  times radio louder than AGNs hosted by disc galaxies, and that the sequences formed by the two populations show similar dependence of the radio-loudness parameter on the Eddington-ratio. This dependence corresponds roughly to constant radio luminosity at  $\lambda > 10^{-3}$  and its drop with the decrease of the Eddington ratio for  $\lambda < 10^{-3}$ . We remind that the elliptical-hosted AGNs are represented in our sample by quasars, BLRGs, and FR I radio galaxies, while the disc-galaxy-hosted AGNs are represented by Seyfert galaxies and LINERS.

The absence of prominent, extended radio structures in AGNs hosted by disc galaxies, when confronted with giant elliptical hosts of the classical double radio sources, led in the past to the conviction that all AGNs in disc galaxies are radio-quiet, and that all AGNs in giant elliptical galaxies are radio-loud. Only recently, after the HST allowed to image and determine the host morphologies of distant, luminous quasars, it has become clear that the claimed one-to-one corre-

spondence between the radio-loudness and the galaxy morphology is invalid: a number of luminous, radio-quiet quasars have been found to be hosted by giant elliptical galaxies (see Floyd et al. 2004 and references therein). This discovery stimulated in turn searches for radio-loud AGNs among those hosted by disc galaxies. Surely, Ho & Peng (2001) demonstrated that after subtraction of the starlight, nuclei of some Seyfert galaxies ‘become’ radio-loud, according to criterion  $\mathcal{R} > 10$  introduced by Kellerman (1989) for quasars. The same was found for LINERS in nearby disc galaxies (Ho 2002). However, as we have shown in this paper, all Seyfert galaxies and LINERS remain well separated from the BLRGs and FR I radio galaxies, and the fact that some of them reach  $\mathcal{R} > 10$  is caused by the increase of the radio-loudness with the decreasing Eddington ratio. Noting such a dependence, we propose to call an AGN radio-loud if

$$\log \mathcal{R} > \log \mathcal{R}^* = \begin{cases} -\log \lambda + 1 & \text{for } \log \lambda > -3 \\ 4 & \text{for } \log \lambda < -3 \end{cases} . \quad (5)$$

## 4.2 AGNs vs BH X-ray binaries

Gallo, Fender, & Pooley (2003) discovered that radio luminosities of BH binaries in low/hard states (i.e., at low accretion rates) correlate with X-ray luminosities,  $L_X$ . They found that luminosity variations of two objects, GX 339-4 and V404 Cyg, follow the relation  $L_R \propto L_X^{0.7}$  which holds over more than three order of magnitudes in  $L_X$  with the same normalization within a factor of 2.5. This discovery triggered speculations that the powering of radio activity in XRBs during the low/hard state is entirely determined by accretion. However, the fact that a similar trend, albeit with a huge scatter, is followed by both our AGN sequences (compare the low- $L_B/L_{\text{Edd}}$  sections in our Figure 2 with Figure 2 from Gallo et al. [2003]) seems to prove that radio-loudness cannot depend only on the accretion rate: an extra parameter is required to explain the bimodal distribution of radio-loudness for spiral-hosted and elliptical-hosted AGNs at low  $\lambda$ ’s, and its significant scatter within both sequences.

The monotonic dependence of radio luminosities on the Eddington ratio in XRBs breaks down at  $\lambda \sim 0.01$ , and observations clearly indicate the intermittency of the jet production at higher luminosities and its connection with a spectral state (Fender, Belloni, & Gallo 2004). Qualitatively a similar break but located at smaller  $\lambda$ ’s is seen in the AGN sequences.

Motivated by the similarities of the low- and high- $\lambda$  patterns in XRBs and AGNs, Merloni, Heinz, & Di Matteo (2003) proposed that at high accretion luminosities the jet production is intermittent also in AGNs. This idea was recently explored and supported by Nipoti, Blundell, & Binney (2005). However, at high accretion rates (just as at the low ones discussed previously)

spiral-hosted AGNs are located exclusively in the radio-quiet sequence of our Figures 1-3, as opposed to quasars which populate both upper and lower patterns. Only few exceptional cases are known in which the high- $\lambda$  spiral-hosted AGNs reach radio-loudness  $\mathcal{R} > 100$  (Véron-Cetty & Véron 2001; Ledlow et al. 2001; Whalen et al. 2006) — all the others objects of this kind are  $\sim 10^3$  times radio weaker than the radio-loud quasars and BLRGs with similar values of  $\lambda$ . Clearly this fact indicates again that an extra parameter must play a role in explaining why the upper, radio-loud sequence in our Figures 1-3 is reachable only by the AGNs hosted by early type galaxies.

### 4.3 The spin paradigm

In the next section we will argue that the black hole spin is the required additional parameter determining radio-loudness of AGNs. Before exploring this possibility, let us first review shortly the past and present day status of the so-called ‘spin paradigm’.

In 1990, Blandford suggested that efficiency of the jet production (assuming that a jet is powered by the rotating black hole via the Blandford-Znajek mechanism) is determined by the black hole spin,  $J$ , or, more precisely, by the dimensionless angular momentum,  $a \equiv J/J_{max} = cJ/GM_{BH}^2$ . This is a very attractive because in principle it can explain the very wide range of radio-loudness of AGNs that look very similar in many other aspects. This spin paradigm was explored by Wilson & Colbert (1995), who assumed that the spin evolution is determined by black-hole mergers. They showed that mergers of black holes which follow mergers of galaxies lead to a broad, ‘heavy-bottom’ distribution of the spin, consistent with a distribution of radio-loudness. This result was challenged by Hughes & Blandford (2003), who demonstrated that the required fraction of the black holes with high spins is not available in the merger scenario, and that accretion must play a key role in black-hole spin-up. However, as noticed earlier by Moderski & Sikora (1996) and Moderski, Sikora & Lasota (1998), spin-up by accretion discs is so efficient, that in order to match the distribution of radio-loudness with the spin distribution, it is necessary to postulate that accretion events lead to formation of both co-rotating and counter-rotating discs, depending on the initial angular momenta. This possibility was recently questioned by Volonteri et al. (2005) who argue that angular momentum coupling between black holes and accretion discs is so strong, that the innermost portions of a disc are always forced to co-rotate with a black hole, and therefore that all AGN black-holes should have large spins.<sup>2</sup>

This sort of arguments, together with the connection of jet production in BH XRBs with dif-

<sup>2</sup> See also in this context Elvis, Risaliti & Zamorani (2002).

ferent spectral states (§4.1), at first glance seem to favor a disc-jet scenario, without the necessity of involving the spin of the central object in the jet launching process. An additional support for this idea is provided by such observational feature as:

(i) very large spin of the central black-hole in the radio-quiet Seyfert galaxy MCG-6-30-15 deduced from the profile of the fluorescent iron line (Wilms et al. 2001);

(ii) the significant content of protons in quasar jets, as deduced from the analysis of blazar spectra (Sikora & Madejski 2000; Sikora et al. 2005), and indicated by discovery of circular polarization in radio cores (Wardle et al. 1998; Homan, Attridge, & Wardle (2001);

(iii) the presence of relativistic jets in the neutron star XRBs (Fomalont, Geldzahler & Bradshaw 2001; Fender et al. 2004).

However, as already argued in a previous section, accretion alone cannot explain the huge scatter of the radio-loudness observed in AGNs over all scales of the Eddington ratios, nor can it explain the dependence of the radio-loudness on the host-galaxy morphology. Below (§4.3) we draw a version of the spin paradigm scenario which explains our main results on the radio-loudness of AGNs, and the same time accommodates the features (i)-(iii) listed above (see §4.4).

#### 4.4 Spin–accretion scenario

If, as in the classical edition of the Blandford-Znajek mechanism, the power of a jet is proportional to  $a^2 B^2$  then, since poloidal magnetic fields are supported in the center by the total pressure of the accretion disc (Moderski & Sikora 1996) or by its  $\alpha$  fraction, where  $\alpha$  is the dimensionless viscosity parameter (Gosh & Abramowicz 1997), the slope of the radio-loudness dependence on the Eddington-ratio is determined by the accretion rate, whereas its normalization — by the value of the black-hole spin. This particularly concerns low Eddington ratios,  $\lambda < 10^{-3}$ . At larger Eddington ratios, processes which suppress efficient jet production can additionally contribute to the observed scatter of radio-loudness. If this is the case, then even for a narrow spin distribution, the radio-loudness at high accretion luminosities can get a broad range, with a bimodal distribution corresponding to two accretion modes, smoothed out due to the finite time scale of transitions between two accretion states. (Obviously, the bimodality can be additionally smoothed out, if the spin distribution is not narrow.) The above picture is likely to apply to AGNs hosted by giant elliptical galaxies: they all can have large spins but show wide range of radio-loudness at high accretion rates because of suppression of a jet production at some states.

We speculate that the above–mentioned radio-loudness bimodality results from intermittency



of narrow-jet production. Since formation of narrow *relativistic* jets requires not only power but also collimation (Begelman & Li 1994), we suggest that the intermittent production of narrow outflows is related to intermittent collimation and that the latter is provided by a surrounding non-relativistic, MHD outflow, launched in the accretion disc. Such a double jet structures were originally proposed by Sol, Pelletier, & Asseo (1989), and shown to provide good collimation by Bogovalov & Tsinganos (2005), Gracia, Tsinganos, & Bogovalov (2005), and Beskin & Nokhrina (2005). Assuming, that at  $\lambda > \lambda_c$  the accretion disc has two realizations, being driven alternatively by viscous forces or by magnetic torques from MHD winds, one can obtain intermissions of the collimation by transitions between these two accretion modes. As Livio, Pringle, & King (2003) suggested and Mayer & Pringle (2006) confirmed, the transitions can be led by processes responsible for generation of a poloidal magnetic field. An alternative scenario, proposed by Spruit & Uzdensky (2005), involves a drift of isolated patches of magnetic fields to the center from very large distances.

Explaining the bimodality of radio-loudness connected with the host galaxy morphology is a greater challenge. In terms of the spin paradigm the much lower radio-loudness of AGNs hosted by disc galaxies indicate much lower spins of their central black-holes. One must explain why in an accretion-dominated evolution, black holes in disc galaxies are protected against spinning up, whereas their counterparts in elliptical galaxies are not.

First, one should stress that the strength of angular-momentum coupling between a black hole and an accretion disc is model-dependent and, for example, as was demonstrated by King et al. (2005) and confirmed by Lodato & Pringle (2006), retrograde accretion discs can be formed if the initial misalignment between the dominant black-hole angular-momentum and the disc angular-momentum is larger than 90 degrees. Nevertheless scenarios based on this possibility cannot explain the radio bimodality of the two AGN populations.

A more promising idea is based on the fact that for a very slowly rotating black hole the time scale of the Lense-Thirring precession is so long that the disc will not be warped at all remaining down to its inner edge misaligned with the equatorial plane of the black hole. This will happen if the black-hole spin is smaller than

$$a_c = \frac{2^{1/2}}{\alpha} \left(\frac{H}{R}\right)^2 \left(\frac{r_{in}}{r_s}\right)^{3/2} \sim 0.1 \frac{(30H/R)^2}{(\alpha/0.1)} \left(\frac{r_{in}}{3r_s}\right)^{3/2} \quad (6)$$

(Volonteri et al. 2005), where  $H/R$  is the aspect ratio of the accretion disc,  $r_{in}$  the radius of its inner edge, and  $r_s$  is the Schwarzschild radius. Hence, if the accretion history of a black hole is made only of small accretion events with a random sequence of the angular-momentum orientations, and

if its initial spin is small (for example when at early epochs black holes were fed by capture of material from tidally disrupted stars; Milosavljević, Merritt, & Ho 2006), then the threshold value  $a_c$  will never be reached. But if the history at some moment was marked by a major merger, the spin can jump up to at least a moderate value due to a merger of two black holes with not very different masses and/or accretion of a large portion of matter with the same angular momentum orientation. All later accretion events will continue to spin up a black hole provided the condition  $a > a_c$  is satisfied. Noting now that most, if not all, progenitors of giant elliptical galaxies undergo major mergers, while disc galaxies probably not (see, e.g., Hopkins et al. 2006), it is likely that only in giant elliptical galaxies the spin of an evolving black holes can cross the threshold value and then make its way to maintain  $a \simeq 1$ .

In black-hole XRBs the situation is simpler: since to reach the maximum spin a black hole has to double its mass, black-hole spins in low-mass binaries do not evolve during the lifetime of the systems. Therefore one should not expect in this case the presence of two radio-loudness sequences as observed (Gallo et al. 2003). Observations suggest ‘moderate’ black-hole spin values in several XRBs (see e.g. Schafee et al. 2006 and Davis, Done & Blaes 2006) so in principle they would be equivalent to the “radio-loud” AGN sequence.

#### **4.5 Protons in quasar jets; neutron star XRBs; Seyfert galaxy MCG-6-30-15**

Let us address now the remaining arguments used in literature against the spin paradigm, and listed by us in the subsection §4.2.

*(i) The Seyfert galaxy MCG 6-30-15:*

The interpretation of the very extended and weak red wing of the fluorescent iron line observed in radio-quiet Seyfert galaxy MCG 6-30-15 in terms of the model involving rapid rotation of the central black hole (Wilms et al. 2001) is not unique, and depends crucially on the details of the continuum production in the vicinity of the black hole. These details are very uncertain (Beckwith & Done 2004). Furthermore, broad fluorescent iron lines can be produced also in the wind (Done & Gierliński 2006). If, however, the black hole in MCG 6-30-15 is indeed spinning rapidly, then the discussed object may be simply exceptional for its class. We emphasize in this context, that the main ingredient of our spin-accretion paradigm stating that disc galaxy-hosted AGNs have slowly spinning black holes, has only a statistical meaning. In fact, MCG 6-30-15 radiates at the rate corresponding to  $\lambda > 10^{-3}$ . Thus the probability of picking it up as a radio-loud object is about ten times smaller than as a radio-quiet one.

*(ii) Protons in quasar jets:*

Theories of jet launching by rotating black holes predict a zero proton content (see particular models by Hawley & Krolik 2006; McKinney 2006; and refs. therein). This is because proton loading near the black hole is protected by the magnetic fields threading the black hole horizon (note that Larmor radius of non-relativistic protons is many orders of magnitude smaller than the size of an AGN jet base). However, jets can be loaded by protons following an interchange instabilities operating at the interface between the central (relativistic) and the external (non-relativistic) outflows (see Sect. 4.4). If both these outflows are Poynting flux dominated, then only the non-relativistic one is efficiently self-collimated. Therefore the two outflows press against each other resulting in mass exchange. Additionally, both the components are subject to kink (and other types of MHD) instabilities, which can increase the mass exchange rate. Unfortunately, no quantitative model exists to show whether efficient proton loading can be provided in this way. An alternative possibility is that the central, relativistic outflow is launched by the innermost portions of an accretion disc. Since the disc's parameters in the very central region depend strongly on the black hole spin, it is possible that the dependence of a jet power on the black hole spin is simply due to larger efficiency of a jet production in the case of a matter accreting onto rapidly rotating black hole. As pointed out by Sikora et al. (2005), also in this case the central portion of a jet can be relativistic, provided magnetic field lines are at small angles to the disc axis.

*(iii) Neutron star XRBs:*

The discovery of relativistic jets in XRB systems with neutron stars proves that the existence of an ergosphere, which plays a key role in an extraction of a black hole rotational energy, is not necessary for producing relativistic jets. Does it contradict with the proposed spin paradigm? Let us recall that the condition for launching a Poynting-flux dominated outflow, which later becomes converted to the matter dominated relativistic jet, is to supply a high magnetic-to-rest-mass energy ratio ( $\gg 1$ ) at the base of the outflow. But this condition is obviously satisfied in the case of the magnetic field anchored on a neutron star. Moreover, as in the black-hole systems, slower winds from the accretion disc can collimate the central portion of the outflow launched from the rotating neutron star. Such a scenario provides natural explanation for an abrupt drop of jet radio luminosities in neutron star XRBs below a certain X-ray luminosity (see Fig.3 in Migliari & Fender 2006): since the magnetic field anchored on a neutron star does not depend on the accretion rate, while the magnetic field in the disc does, the collimation of the outflow from a neutron star by a wind from the disc breaks below a given accretion rate. Of course, the lower the neutron-star magnetic field, the lower the accretion luminosity at the break, which can explain why millisecond

accreting XRB pulsars are detected in radio even at very low accretion luminosities (see Fig.2 in Migliari & Fender 2006).

## 5 CONCLUSIONS

The main conclusions of our studies are:

- the upper boundaries of radio-loudness of AGNs hosted by giant elliptical galaxies are by  $\sim 3$  orders of magnitude larger than upper boundaries of radio-loudness of AGNs hosted by disc galaxies;
- both populations of spiral-hosted and elliptical-hosted AGNs show a similar dependence of the upper bounds of the radio loudness parameter  $\mathcal{R}$  on the Eddington ratio  $\lambda$ : the radio loudness increases with the decreasing Eddington ratio at the high accretion rates  $\lambda \gtrsim 10^{-3}$ , and saturates at smaller  $\lambda$ 's; this dependence corresponds to roughly constant radio luminosities at large accretion luminosities, and (not necessarily linear) correlation with the Eddington ratio at smaller accretion luminosities;
- the huge, host-morphology-related difference between the radio-loudness reachable by AGNs in disc and elliptical galaxies can be explained by the scenario according to which
  - (i) it is the spin of a black hole which controls jet production processes (in neutron star XRBs it is be the neutron star rotation),
  - (ii) central black holes can reach large spins only in early type galaxies (following major mergers), and not (in a statistical sense) in spiral galaxies.

## ACKNOWLEDGMENTS

M.S. was partially supported by Polish MEiN grant 1 P03D 00928 and in 2005 by a CNRS “poste rouge” at IAP. Ł.S. acknowledges support by MEiN grant 1 P03D 00329 and by the ENIGMA Network through the grant HPRN-CT-2002-00321. Ł.S. thanks the Fellows of the IAP for their hospitality and support during his stays there. JPL was supported in part by a grant from the CNES.

## REFERENCES

- Becker, R.H., White, R.L., & Edwards, A.L. 1991, *ApJS*, 75, 1  
 Becker, R.H., White, R.L., & Helfand, D.J. 1995, *ApJ*, 450, 559  
 Beckwith, K., & Done, C. 2004, *MNRAS*, 352, 353

- Beskin, V.S., & Nokhrina, E.E. 2005, astro-ph/0509064
- Blandford, R.D. 1990, in *Active Galactice Nuclei*, ed. T.J.-L. Courvoisier & M. Mayor (Saas-Fee Advanced Course 20)(Berlin:Spronger), 161
- Bogovalov, S., & Tsinganos, K. 2005, MNRAS, 357, 918
- Cao, X., & Rawlings, S. 2004, MNRAS, 349, 1419
- Chiaberge, M., Capetti, A., & Celotti, A. 1999, A&A, 349, 77
- Chiaberge, M., Capetti, A., & Macchetto, F.D. 2005, ApJ, 625, 716
- Cirasuolo, M., Magliocchrtti, M., Celotti, A., & Danese, L. 2003, MNRAS, 341, 993
- Cirasuolo, M., Celotti, A., Magliocchrtti, M., & Danese, L. 2003, MNRAS, 346, 447
- Condon, J.J., Cotton, W.D., Greissen, E.W., et al. 1998, AJ, 115, 1693
- Croom, S.M., Smith, R.J., Boyle, B.J., et al. 2001, MNRAS, 322, L29
- Done, C., & Gierliński, M. 2006, MNRAS, in press [astro-ph/0510614]
- Davis, S. W., Done, C., & Blaes, O. M. 2006, astro-ph/0602245
- Elvis, M., Risaliti, G., & Zamorani, G., 2002, ApJ, 565, L75
- Eracleous, M., & Halpern, J.P. 1994, ApJS, 90, 1
- Eracleous, M., & Halpern, J.P. 2004, ApJS, 150, 181
- Feigelson, E.D., Maccacaro, T., & Zamorani, G. 1982, ApJ, 255, 392
- Fender, R.P. 2004, astro-ph/030339
- Fender, R.P., Belloni, T.M., & Gallo, E. 2004, MNRAS, 355, 1105
- Fender, R., Wu, K., Johnston, H., et al. 2004, Nature, 427, 222
- Floyd, D.J.E., Kukula, M.J., Dunlop, J.S., et al. 2004, MNRAS, 355, 196
- Fomalont, E.B., Geldzahler, B.J., & Bradshaw, C.F. 2001, ApJ, 558, 283
- Gallo, E., Fender, R.P., & Pooley, G.G. 2003, MNRAS, 344, 60
- Ghosh, P., Abramowicz, M. 1997, MNRAS, 292, 887
- Gracia, J., Tsinganos, K., & Bogovalov, S.V. 2005, A&A, 442, L7
- Gregory, P.C., & Condon, J.J. 1991, ApJS, 75, 1011
- Haas, M., Müller, S.A.H., Bertoldi, F., et al. 2004, A&A, 424, 531
- Hawley, J.F., & Krolik, J.H. 2006, ApJ, in press (astro-ph/0512227)
- Ho, L.C. 1999, ApJ, 516, 672
- Ho, L.C. 2002, ApJ, 564, 120
- Ho, L.C., & Peng, C.Y. 2001, ApJ, 555, 650
- Homan, D.C., Attridge, J.M., & Wardle, J.F.C. 2001, ApJ, 556, 113
- Hopkins, P.F., Bundy, K., Hernquist, L., & Ellis, R.S. 2006, ApJ, submitted (astro-ph/0601621)

- Hughes, S.A., & Blandford, R.D. 2003, *ApJ*, 585, L101
- Ivezić, Ž, Menou, K., Knapp, G.R., et al. 2002, *AJ*, 124, 2364
- Kellermann, K.I., Sramek, R., Schmidt, M., et al. 1989, *AJ*, 98, 1195
- Kharb, P., & Shastri, P. 2004, *A&A*, 425, 825
- King, A.R., Lubow, S.H., Ogilvie, G.I., & Pringle, J.E. 2005, *MNRAS*, 363, 49
- Knapp, G.R., Bies, W.E., & van Gorkom, J.H. 1990, *AJ*, 99, 476
- Komossa, S., Voges, W., Xu, D., et al. 2006, astro-ph/0603680
- Kühr, H., Witzel, A., Pauliny-Toth, I.I.K., & Nauber, U. 1981, *A&AS*, 45, 367
- Laor, A., 2003, *ApJ*, 590, 86
- Ledlow, M.J., Owen, F.N., Yun, M.S., & Hill, J.M. 2001, *ApJ*, 552, 120
- Livio, M., Pringle, J.E., & King, A.R. 2003, *ApJ*, 593, 184
- Lodato, G., & Pringle, J.E. 2006, astro-ph/0602306
- Mayer, M., & Pringle, J.E. 2006, *MNRAS*, accepted (astro-ph/0601663)
- McKinney, J.C. 2006, astro-ph/0603045
- Merloni, A., Heinz, S., & Di Matteo, T. 2003, *MNRAS*, 345, 1057
- McLure, R.J., & Jarvis, M.J. 2004, *MNRAS*, 353, L45
- Migliari, S., & Fender, R.P. 2006, *MNRAS*, 366, 79
- Miller, L., Peacock, J.A., & Mead, A.R.G. 1990, *MNRAS*, 244, 207
- Milosavljević, M., Merritt, D., & Ho, L.C. 2006, astro-ph/0602289
- Moderski, R., & Sikora, M. 1996, *MNRAS*, 283, 854
- Moderski, R., Sikora, M., & Lasota, J.-P. 1998, *MNRAS*, 301, 142
- Müller, S.A.H., Haas, M., Siebenmorgen, R., et al. 2004, *A&A*, 426, L29
- Nagar, N.M., Falcke, H., & Wilson, A.S. 2005, *A&A*, 435, 521
- Nipoti, C., Blundell, K.M., & Binney, J. 2005, *MNRAS*, 361, 633
- Pedlar, A., Ghataure, H.S., Davies, R.D., et al. 1990, *MNRAS*, 246, 477
- Richards, G.T., Lacy, M., Storrie-Lombardi, L.J., et al. 2006, astro-ph/0601558
- Shafee, R., McClintock, J. E., Narayan, R., Davis, S. W., Li, L.-X., & Remillard, R. A. 2006, *ApJ*, 636, L113
- Schmidt, M., & Green, R.F., 1983, *ApJ*, 269, 352
- Sikora, M., Begelman, M.C., Madejski, G.M., & Lasota, J.-P. 2005, *ApJ*, 625, 72
- Sikora, M., & Madejski, G.M. 2000, *ApJ*, 534, 109
- Spruit, H.C., & Uzdensky, D.A. 2005, *ApJ*, 629, 960
- Stoche, J.T., Morris, S.L., Weymann, R.J., et al. 1992, *ApJ*, 396, 487

- Strateva, I.V., Strauss, M.A., Hao, L., et al. 2003, *AJ*, 126, 1720
- Strittmatter, P.A., Hill, P., Pauliny-Toth, I.I.K., et al. 1980, *A&A*, 1980, 88, L12
- Tully, R.B., 1988, *Nearby Galaxies Catalog* (Cambridge: Cambridge Univ. Press)
- Ulvestad, J.S., Antonucci, R.R.J., & Goodrich, R.W. 1995, *AJ*, 109, 81
- Verdoes Kleijn, G.A., Baum, S.A., de Zeeuw, P.T. 2002, *AJ*, 123, 1334
- Véron-Cetti, M.-P., & Véron, P. 1989, *ESO Scientific Rep. No. 7, A Catalog of Quasars and Active Nuclei* (4th ed.; München: ESO)
- Véron-Cetti, M.-P., & Véron, P. 2001, *A&A*, 375, 791
- Vestergaard, M. 2002, *ApJ*, 571, 733
- Volonteri, M., Madau, P., Quataert, E., & Rees, M.J. 2005, *ApJ*, 620, 69
- Wardle, J.F.C., Homan, D.C., Ojha, R., et al. 1998, *Nature*, 395, 457
- Whalen, D.J., Laurent-Muehleisen, S.A., Moran, E.C., & Becker, R.H. 2006, *AJ*, to appear
- White, R.L., & Becker, R.H. 1992, *ApJS*, 79, 331
- White, R.L., Becker, R.H., Gregg, M.D., et al. 2000, *ApJS*, 126, 133
- Wilms, J., Reynolds, C.S., Begelman, M.C., et al. 2001, *MNRAS*, 328, L27
- Wilson, A.S., & Colbert, E.J.M. 1995, *ApJ*, 438, 62
- Woo, J.-H., & Urry, C.M. 2002, *ApJ*, 579, 530
- Wright, A.E., Griffith, M.R., Burke, B.F., & Ekers, R.D. 1994, *ApJS*, 91, 111
- Wright, A.E., & Otrupcek, R. 1990, *Parkes Catalog 1990, Australia Telescope National Facility*
- Wu, X.-B., & Liu, F.K. 2004, *ApJ*, 614, 91
- York, D.G., Adelman, J., Anderson, J.E., Jr., et al. 2000, *AJ*, 120, 1579
- Zhou, H. & Wang, T. 2002, *ChJAA*, 2, 501
- Zirbel, E.L., & Baum, S.A. 1995, *ApJ*, 448, 521

## **APPENDIX A: TABLES**

**Table A1. Broad-Line Radio Galaxies.** Reference in column 9: [1] Wright & Orupcek (1990), [2] Gregory & Condon (1991), [3] Condon et al. (1998), [4] Feigelson et al. (1982), [5] Kühr et al. (1981), [6] Becker et al. (1995), [7] Wright et al. (1994), [8] Becker et al. (1991).

IAU J2000.0 (1)	name (2)	$z$ (3)	$m_V$ (4)	$A_V$ (5)	$\kappa_*$ (6)	$\log L_B$ [erg/s] (7)	$F_5$ [Jy] (8)	ref. to col. 8 (9)	$\log L_R$ [erg/s] (10)	$\log \mathcal{R}$ (11)	$FWHM_{H\alpha}$ [km/s] (12)	$\log \mathcal{M}_{BH}$ [ $\mathcal{M}_\odot$ ] (13)	$\log L_B$ [ $L_{Edd}$ ] (14)	$\log L_R$ [ $L_{Edd}$ ] (15)
0038-0207	3C 17	0.22	18	0.08	0.58	43.9	2.48	1	43.2	4.45	11500	8.7	-2.9	-3.6
0044+1211	4C +11.06	0.226	19	0.26	0.28	43.8	0.22	1	42.2	3.49	4299	7.8	-2.1	-3.7
0207+2931	3C 59	0.11	16	0.21	0.28	44.4	0.67	2	42.0	2.78	9800	8.9	-2.6	-5.0
0224+2750	3C 67	0.311	18.6	0.42	0.82	43.8	0.87	2	43.1	4.48	6200	8.1	-2.4	-3.1
0238-3048	IRAS 02366-3101	0.062	15	0.22	0.3	44.2	0.00343	3	39.2	0.10	7800	8.6	-2.5	-7.5
0238+0233	PKS 0236+02	0.207	17.7	0.11	0.46	44.1	0.12	1	41.9	2.89	11200	8.8	-2.8	-5.1
0312+3916	B2 0309+39	0.161	18.2	0.49	0.1	44.0	0.822	2	42.5	3.55	6300	8.3	-2.4	-3.9
0342-3703	PKS 0340-37	0.285	18.6	0.03	0.19	44.2	0.71	1	42.9	3.89	9800	8.8	-2.7	-3.9
0343+0457	3C 93	0.357	19.2	0.8	0.43	44.3	0.91	1	43.3	4.09	19600	9.5	-3.3	-4.3
0452-1812	MS 0450.3-1817	0.059	17.8	0.14	0.9	42.2	0.0026	4	39.0	1.97	10900	7.5	-3.4	-6.6
0519-4546	Pictor A	0.035	16.2	0.14	0.14	43.3	15.54	5	42.3	4.17	18400	8.7	-3.5	-4.5
0832+3707	CBS 74	0.092	16	0.12	0.17	44.2	0.00424	6	39.6	0.56	9200	8.7	-2.6	-7.2
0849+0949	PKS 0846+101	0.365	19.2	0.19	0.11	44.3	0.1	1	42.3	3.18	9600	8.8	-2.7	-4.6
0859-1922	PKS 0857-191	0.361	19.7	0.69	0	44.3	0.4	1	42.9	3.73	6500	8.5	-2.3	-3.7
0914+0507	4C +05.38	0.302	17.4	0.17	0.51	44.6	0.22	1	42.5	3.06	10600	9.1	-2.7	-4.7
0923-2135	PKS 0921-213	0.053	16.5	0.2	0.65	43.2	0.42	1	41.1	3.09	8300	7.9	-2.9	-4.9
0947+0725	3C 227	0.086	16.3	0.09	0.4	43.9	2.6	1	42.4	3.62	13900	8.9	-3.1	-4.6
1030+3102	B2 1028+31	0.178	16.7	0.27	0.18	44.6	0.172	2	41.9	2.40	6400	8.7	-2.2	-4.9
1154-3505	PKS 1151-34	0.258	17.8	0.28	0.75	44.0	2.74	1	43.4	4.56	13400	8.9	-3.0	-3.6
1257-3334	PKS 1254-333	0.19	18.6	0.28	0.22	43.9	0.54	1	42.4	3.68	6300	8.2	-2.4	-3.9
1332+0200	3C 287.1	0.216	18.3	0.08	0.36	44.0	1.35	1	43.0	4.12	4700	8.0	-2.1	-3.1
1407+2827	Mrk 0668	0.077	15.4	0.06	0.27	44.2	2.421	2	42.2	3.15	6000	8.4	-2.3	-4.2
1419-1928	PKS 1417-19	0.12	16.7	0.28	0.05	44.3	0.83	1	42.2	3.01	4900	8.3	-2.1	-4.2
1443+5201	3C 303	0.141	17.3	0.06	0.73	43.6	1.044	2	42.4	3.99	6800	8.0	-2.6	-3.7
1516+0015	PKS 1514+00	0.053	15.6	0.18	0.76	43.4	1.37	1	41.7	3.42	4300	7.5	-2.2	-3.9
1533+3544	4C +35.37	0.157	17.8	0.08	0	44.1	0.129	2	41.6	2.70	4300	8.0	-2.0	-4.5
1617-3222	3C 332	0.151	16	0.08	0.85	43.9	0.92	2	42.4	3.66	23200	9.3	-3.5	-5.0
1637+1149	MC2 1635+119	0.147	16.5	0.17	0.14	44.5	0.051	2	41.2	1.81	4900	8.4	-2.0	-5.3
1719+4858	Arp 102B	0.024	14.8	0.08	0.86	42.7	0.159	2	40.0	2.43	16000	8.2	-3.6	-6.3
1742+1827	PKS 1739+184	0.186	17.5	0.21	0.11	44.3	0.39	1	42.3	3.06	13600	9.2	-2.9	-5.0
1835+3241	3C 382	0.058	15.4	0.23	0.06	44.1	2.281	2	42.0	2.95	11800	8.9	-2.9	-5.1
1842+7946	3C 390.3	0.056	15.4	0.24	0.31	44.0	4.45	5	42.2	3.37	11900	8.8	-2.9	-4.7
2101-4219	PKS 2058-425	0.223	17.2	0.13	0	44.6	0.71	1	42.7	3.19	4600	8.4	-1.9	-3.8
2223-0206	3C 445	0.056	15.8	0.27	0.33	43.8	2.12	1	41.9	3.20	5600	8.0	-2.3	-4.3
2303-1841	PKS 2300-18	0.129	17.8	0.11	0.14	43.8	0.89	1	42.3	3.59	8700	8.4	-2.7	-4.2
2307+1901	PKS 2305+188	0.313	17.5	0.44	0.56	44.6	0.44	1	42.8	3.34	4400	8.4	-1.9	-3.7
2330+1702	MC3 2328+167	0.28	18.3	0.15	0.37	44.2	0.078	2	42.0	2.87	3200	7.8	-1.7	-4.0



**Table A.2. Radio-Loud Quasars.** Reference in column 9: [1] Wright & Otrupcek (1990), [2] Gregory & Condon (1991), [3] Condon et al. (1998), [4] Feigelson et al. (1982), [5] Kuhl et al. (1981), [6] Becker et al. (1995), [7] Wright et al. (1994), [8] Becker et al. (1991).

IAU J2000.0 (1)	name (2)	$z$ (3)	$m_V$ (4)	$A_V$ (5)	$\kappa_*$ (6)	$\log L_B$ [erg/s] (7)	$F_5$ [Jy] (8)	ref. to col. 8 (9)	$\log L_R$ [erg/s] (10)	$\log \mathcal{R}$ (11)	$FWHM_{H\alpha}$ [km/s] (12)	$\log \mathcal{M}_{BH}$ [ $M_\odot$ ] (13)	$\log L_B$ [ $L_{Edd}$ ] (14)	$\log L_R$ [ $L_{Edd}$ ] (15)
0019+2602	4C 25.01	0.284	15.4	0.1	0	45.6	0.405	2	42.7	2.24	4600	9.1	-1.6	-4.5
0113+2958	B2 0110+29	0.363	17	0.21	0	45.2	0.311	2	42.8	2.73	7200	9.2	-2.1	-4.5
0157+3154	4C 31.06	0.373	18	0.18	0.11	44.8	0.394	2	43.0	3.30	9000	9.1	-2.4	-4.3
0202-7620	PKS 0202-76	0.389	16.9	0.17	0	45.3	0.8	1	43.3	3.12	6400	9.2	-2.0	-4.0
0217+1104	PKS 0214+10	0.408	17	0.36	0.01	45.4	0.46	1	43.1	2.85	4500	8.9	-1.7	-3.9
0311-7651	PKS 0312-77	0.225	16.1	0.32	0	45.2	0.59	1	42.6	2.59	2900	8.4	-1.3	-3.9
0418+3801	3C 111	0.049	18	5.46	0.04	45.1	6.637	2	42.3	2.35	4800	8.8	-1.8	-4.6
0559-5026	PKS 0558-504	0.138	15	0.15	0	45.1	0.121	7	41.5	1.52	1000	7.4	-0.4	-4.1
0745+3142	B2 0742+31	0.462	16	0.23	0	45.9	0.957	2	43.5	2.82	6500	9.6	-1.8	-4.2
0815+0155	PKS 0812+02	0.402	17.1	0.1	0.01	45.2	0.77	1	43.3	3.22	4600	8.8	-1.7	-3.6
0839-1214	3C 206	0.197	15.8	0.15	0	45.1	0.72	1	42.6	2.63	5100	8.8	-1.9	-4.4
0927-2034	PKS 0925-203	0.347	16.4	0.19	0	45.4	0.7	1	43.1	2.85	2200	8.3	-1.0	-3.3
0954+0929	4C +09.35	0.298	17.2	0.11	0	44.9	0.18	1	42.4	2.61	5100	8.7	-1.9	-4.4
1006-4136	PKS 1004-217	0.33	16.9	0.2	0	45.2	0.3	1	42.7	2.68	2100	8.1	-1.1	-3.5
1007+1248	PKS 1004+13	0.24	15.2	0.13	0	45.5	0.42	1	42.5	2.16	6100	9.3	-1.9	-4.9
1013-2831	PKS 1011-282	0.255	16.9	0.21	0	44.9	0.29	1	42.4	2.65	4100	8.5	-1.7	-4.2
1022-1037	PKS 1020-103	0.197	16.1	0.15	0	45.0	0.49	1	42.4	2.58	8700	9.2	-2.4	-4.9
1051-0918	3C 246	0.345	16.8	0.14	0	45.2	0.7	1	43.1	3.03	6300	9.1	-2.0	-4.1
1103-3251	PKS 1101-325	0.355	16.5	0.31	0	45.4	0.73	2	43.2	2.86	3500	8.8	-1.4	-3.7
1107+3616	B2 1104+36	0.392	18	0.06	0	44.8	0.217	2	42.7	3.04	6800	8.9	-2.2	-4.3
1131+3114	B2 1128+31	0.29	16	0.07	0.01	45.3	0.31	1	42.6	2.39	4000	8.8	-1.6	-4.3
1148-0404	PKS 1146-037	0.341	16.9	0.11	0.5	44.9	0.34	2	42.8	3.07	5000	8.7	-1.9	-4.0
1153+4931	LB 2136	0.333	17.1	0.07	0	45.0	0.702	2	43.1	3.18	4400	8.7	-1.7	-3.7
1159+2106	TXS 1156+213	0.347	17.5	0.09	0.43	44.7	0.085	2	42.2	2.66	7600	8.9	-2.3	-4.8
1210+3157	B2 1208+32A	0.389	16.7	0.06	0	45.3	0.16	2	42.6	2.39	5900	9.1	-1.9	-4.7
1225+2458	B2 1223+25	0.268	17.1	0.07	0	44.8	0.138	2	42.2	2.47	5400	8.7	-2.0	-4.7
1235-2512	PKS 1233-24	0.355	17.2	0.32	0	45.2	0.61	1	43.1	3.06	4900	8.9	-1.8	-3.9
1252+5624	3C 277.1	0.32	17.9	0.04	0	44.7	0.883	2	43.1	3.61	3200	8.1	-1.6	-3.1
1305-1033	PKS 1302-102	0.278	15.2	0.14	0	45.7	1	1	43.1	2.54	3400	8.9	-1.3	-3.9
1349-1132	PKS 1346-112	0.341	18	0.21	0	44.8	0.58	1	43.0	3.40	2300	7.9	-1.3	-3.0
1353+2631	B2 1351+26	0.308	17.2	0.05	0.1	44.9	0.098	2	42.2	2.42	7800	9.1	-2.3	-5.0
1359-4152	PKS 1355-41	0.314	15.9	0.29	0.05	45.5	1.4	1	43.3	2.93	9800	9.7	-2.3	-4.5
1423-5055	CSO 0643	0.276	16.7	0.04	0.28	44.9	0.225	2	42.4	2.68	9000	9.2	-2.4	-4.9
1454-3747	PKS 1451-375	0.314	16.7	0.26	0	45.2	1.84	1	43.4	3.36	3800	8.7	-1.6	-3.3
1514+3650	4C +37.43	0.371	16.3	0.07	0.04	45.4	0.361	2	42.9	2.59	7500	9.4	-2.1	-4.6
1527+2233	LB 9743	0.254	16.7	0.18	0	45.0	0.16	2	42.2	2.33	3700	8.5	-1.6	-4.4
1609+1756	4C + 18.47	0.346	18	0.18	0	44.8	0.28	1	42.7	3.10	6100	8.8	-2.1	-4.2

**Table A2. Radio-Loud Quasars - continued.** Reference in column 9: [1] Wright & Orupcek (1990), [2] Gregory & Condon (1991), [3] Condon et al. (1998), [4] Feigelson et al. (1982), [5] Kühr et al. (1981), [6] Becker et al. (1995), [7] Wright et al. (1994), [8] Becker et al. (1991).

IAU J2000.0 (1)	name (2)	$z$ (3)	$m_V$ (4)	$A_V$ (5)	$\kappa_*$ (6)	$\log L_B$ [erg/s] (7)	$F_5$ [Jy] (8)	ref. to col. 8 (9)	$\log L_R$ [erg/s] (10)	$\log \mathcal{R}$ (11)	$FWHM_{H\alpha}$ [km/s] (12)	$\log \mathcal{M}_{BH}$ [ $\mathcal{M}_\odot$ ] (13)	$\log L_B$ [ $L_{Edd}$ ] (14)	$\log L_R$ [ $L_{Edd}$ ] (15)
1704+6044	3C 351	0.372	15.3	0.08	0	45.9	1.258	2	43.5	2.71	1300	8.2	-0.4	-2.9
1721+3542	B2 1719+35	0.283	17.5	0.14	0.14	44.7	0.877	2	43.0	3.47	6000	8.7	-2.1	-3.8
1723+3417	B2 1721+34	0.205	16.5	0.12	0	44.8	0.65	2	42.6	2.87	2300	8.0	-1.2	-3.5
1728+0427	PKS 1725+044	0.297	17	0.47	0	45.1	1.21	1	43.2	3.21	3300	8.5	-1.5	-3.4
1748+1619	MRC 1745+163	0.392	17.6	0.31	0	45.1	0.146	2	42.6	2.61	4200	8.7	-1.7	-4.2
1917-4530	PKS 1914-45	0.364	16.8	0.27	0.1	45.3	0.18	1	42.6	2.44	9800	9.5	-2.4	-5.1
2142-0437	PKS 2140-048	0.345	18	0.11	0	44.7	0.6	1	43.1	3.46	3900	8.4	-1.7	-3.4
2143+1743	OX +169	0.211	15.7	0.37	0.01	45.3	1.061	8	42.8	2.67	4000	8.8	-1.6	-4.1
2211-1328	PKS 2208-137	0.391	17	0.15	0	45.3	0.53	1	43.1	2.99	4100	8.8	-1.6	-3.8
2230-3942	PKS 2227-399	0.318	17.9	0.06	0	44.7	1.02	1	43.2	3.67	6700	8.8	-2.2	-3.7
2250+1419	PKS 2247+14	0.235	16.9	0.17	0	44.8	1.11	1	42.9	3.25	3500	8.3	-1.6	-3.5
2305-7103	PKS 2302-713	0.384	17.5	0.1	0	45.0	0.15	1	42.6	2.66	4600	8.7	-1.8	-4.3
2351-0109	PKS 2349-01	0.174	15.3	0.09	0.05	45.1	0.68	1	42.4	2.44	5800	9.0	-2.0	-4.6

**Table A3. Seyfert Galaxies and Liners.** References in column 9: [1] Ho (2002), [2] Woo & Urry (2002), [3] Chiaberge et al. (2005), [4] Merloni et al. (2003).

IAU J2000.0 (1)	name (2)	$d$ [Mpc] (3)	$ M_B $ (4)	$\log L_B$ [erg/s] (5)	$\log L_R$ [erg/s] (6)	$\log \mathcal{R}$ (7)	$\log \mathcal{M}_{\text{BH}}$ [ $\mathcal{M}_{\odot}$ ] (8)	ref. to col. 8 (9)	$\log L_B$ [ $L_{\text{Edd}}$ ] (10)	$\log L_R$ [ $L_{\text{Edd}}$ ] (11)
0006+2012	Mrk 335	114.2	18.33	42.9	38.4	0.58	6.8	1	-2.0	-6.6
0123-5848	Fairall 9	214.1	23.28	44.9	39.7	-0.04	7.9	1	-1.1	-6.3
0214-0046	Mrk 590	117.0	16.61	42.2	39.2	2.07	7.3	1	-3.1	-6.2
0242-0000	NGC 1068	14.4	16.47	42.2	39.5	2.46	7.2	1	-3.2	-5.8
0319+4130	NGC 1275	75.1	18.68	43.1	42.2	4.30	8.5	2	-3.6	-4.4
0516-0008	Ark 120	144.2	22.77	44.7	39.2	-0.36	8.3	1	-1.7	-7.2
0742+4948	Mrk 79	97.8	20.08	43.6	38.8	0.35	7.7	1	-2.2	-7.0
0919+6912	NGC 2787	7.5	8.27	38.9	36.4	2.62	7.6	1	-6.8	-9.3
0925+5217	Mrk 110	158.3	19.55	43.4	38.9	0.64	6.7	1	-1.5	-6.0
0955+6903	NGC 3031	3.9	11.73	40.3	37.1	2.01	7.8	1	-5.6	-8.8
1023+1951	NGC 3227	20.6	16.01	42.0	38.0	1.16	7.6	1	-3.7	-7.7
1106+7234	NGC 3516	38.9	17.21	42.5	38.0	0.71	7.4	1	-3.0	-7.4
1139+3154	Mrk 744	41.6	17.56	42.6	37.9	0.45	7.5	3	-3.0	-7.7
1139-3744	NGC 3783	38.5	19.01	43.2	38.4	0.34	7.0	-	-1.9	-6.7
1156+5507	NGC 3982	17.0	11.76	40.3	37.7	2.53	6.1	2	-3.9	-6.5
1157+5527	NGC 3998	14.1	12.95	40.8	38.0	2.42	8.7	1	-6.1	-8.8
1203+4431	NGC 4051	17.0	14.97	41.6	37.4	0.93	6.1	1	-2.7	-6.9
1210+3924	NGC 4151	20.3	19.18	43.3	38.5	0.43	7.2	1	-2.0	-6.7
1215+3311	NGC 4203	14.1	10.58	39.8	36.7	2.00	7.9	1	-6.2	-9.3
1218+2948	Mrk 766	55.4	16.72	42.3	38.4	1.32	6.6	4	-2.4	-6.3
1218+4718	NGC 4258	7.3	8.17	38.8	38.0	4.34	7.6	1	-6.9	-7.7
1225+1239	NGC 4388	16.8	13.17	40.8	38.0	2.33	6.8	4	-4.1	-6.9
1236+2559	NGC 4565	9.7	10.19	39.7	37.6	3.04	7.7	4	-6.2	-8.3
1237+1149	NGC 4579	16.8	12.81	40.7	38.0	2.45	7.9	4	-5.3	-8.0
1239-0520	NGC 4593	39.5	17.8	42.7	37.4	-0.13	6.9	1	-2.3	-7.6
1242+1315	NGC 4639	16.8	10.97	40.0	37.1	2.29	6.6	3	-4.7	-7.6
1313+3635	NGC 5033	18.7	14.53	41.4	38.0	1.72	7.5	3	-4.2	-7.6
1338+0432	NGC 5252	98.9	14.38	41.3	39.0	2.83	8.0	2	-4.8	-7.1
1342+3539	NGC 5273	21.3	13.51	41.0	36.8	0.95	6.5	2,3	-3.6	-7.8
1349-3018	IC 4329A	70.2	19.4	43.3	39.0	0.81	6.7	1	-1.5	-5.8
1353+6918	Mrk 279	135.6	20.7	43.9	38.9	0.18	7.6	1	-1.9	-6.8
1417+2508	NGC 5548	75.2	17.44	42.6	38.7	1.25	8.1	1	-3.6	-7.5
1436+5847	Mrk 817	140.4	18.96	43.2	38.8	0.76	7.6	1	-2.6	-7.0
1504+1026	Mrk 841	156.0	18.19	42.9	39.0	1.26	8.1	2	-3.4	-7.2
1531+0727	NGC 5940	145.2	18.27	42.9	38.7	0.99	7.7	2,3	-2.9	-7.1
1616+3542	NGC 6104	119.9	16.32	42.1	38.4	1.41	7.6	2	-3.6	-7.3
2044-1043	Mrk 509	154.1	22.63	44.6	39.2	-0.34	7.8	1	-1.2	-6.7
2303+0852	NGC 7469	71.4	17.93	42.8	39.3	1.72	6.8	1	-2.2	-5.6
2318+0014	Mrk 530	124.2	16.42	42.1	39.0	2.02	8.1	3	-4.1	-7.2

**Table A4. FR I Radio Galaxies.** References in column 6: [1] Wright & Otrupcek (1990), [2] Gregory & Condon (1991), [3] White & Becker (1992), [4] Kuhr et al. (1981). References in column 10: [1] Cao & Rawlings (2004), [2] Woo & Urry (2002).

IAU J2000.0 (1)	name (2)	$z$ (3)	$\log L_B$ [erg/s] (4)	$F_5$ [Jy] (5)	ref. to col. 5 (6)	$\log L_R$ [erg/s] (7)	$\log \mathcal{R}$ (8)	$\log \mathcal{M}_{BH}$ [ $\mathcal{M}_\odot$ ] (9)	ref. to col. 9 (10)	$\log L_B$ [ $L_{Edd}$ ] (11)	$\log L_R$ [ $L_{Edd}$ ] (12)
0055+2624	3C 28	0.1952	<41.4	0.15	1	41.9	>5.63	8.1	1	<-4.8	-4.3
0057-0123	3C 29	0.0448	41.3	2.01	1	41.7	5.51	9.1	1	-5.9	-5.5
0057+3021	NGC 315	0.0167	41.0	0.914	2	40.5	4.55	8.9	2	-6.0	-6.6
0107+32224	3C 31	0.0169	40.9	1.12	2	40.6	4.76	8.6	1	-5.8	-6.2
0123+3315	NGC 507	0.0164	<39.5	0.055	3	39.2	>4.86	9	2	<-7.6	-7.9
0125-0120	3C 40	0.018	<40.5	1.78	1	40.8	>5.46	7.9	2	<-5.5	-5.2
0156+0537	NGC 741	0.0185	<40.2	0.28	1	40.0	>4.96	8.7	2	<-6.6	-6.8
0223+4259	3C 66B	0.0215	41.5	1.77	2	41.0	4.63	8.5	1	-5.1	-5.6
0308+0406	3C 78	0.0288	42.5	3.45	1	41.5	4.13	8.9	1	-4.5	-5.5
0318+4151	3C 83.1	0.0251	40.2	3.034	4	41.3	6.30	8.8	1	-6.7	-5.6
0319+4130	3C 84	0.0176	42.9	42.37	2	42.2	4.42	9.1	1	-4.3	-5.0
0334-0110	3C 89	0.1386	<40.9	0.72	1	42.3	>6.52	8.6	1	<-5.8	-4.5
1145+1936	3C 264	0.0206	42.0	2.36	1	41.1	4.18	8.3	1	-4.4	-5.4
1219+0549	3C 270	0.0074	39.4	4.86	1	40.5	6.20	8.6	1	-7.3	-6.2
1225+1253	3C 272.1	0.0037	40.0	2.72	1	39.6	4.73	8.2	1	-6.3	-6.7
1230+1223	3C 274	0.0037	41.0	67.6	1	41.0	5.12	9.5	1	-6.6	-6.6
1259+2757	NGC 4874	0.0239	<39.3	0.084	2	39.7	>5.52	8.6	2	<-7.4	-7.0
1338+3851	3C 288	0.246	42.0	1.008	2	42.9	6.11	8.9	1	-5.0	-4.1
1416+1048	3C 296	0.0237	40.5	1.202	2	40.9	5.52	8.8	1	-6.4	-6.0
1504+2600	3C 310	0.054	41.3	1.26	1	41.6	5.52	8	1	-4.9	-4.5
1510+7045	3C 314.1	0.1197	<41.4	0.337	2	41.8	>5.51	7.8	1	<-4.5	-4.1
1516+0701	3C 317	0.0342	41.4	0.93	1	41.1	4.88	9.5	1	-6.3	-6.5
1628+3933	3C 338	0.0303	41.2	0.477	2	40.7	4.65	9.1	1	-6.0	-6.5
1643+1715	3C 346	0.162	43.1	1.39	2	42.7	4.74	8.8	1	-3.8	-4.2
1651+0459	3C 348	0.154	41.6	9.529	2	43.5	7.03	8.9	1	-5.4	-3.5
2048+0701	4C 424	0.127	<41.7	0.785	2	42.2	>5.68	8.3	1	<-4.7	-4.2
2155+3800	3C 438	0.29	<41.9	1.703	2	43.3	>6.58	8.6	1	<-4.8	-3.4
2214+1350	3C 442	0.0262	40.0	0.76	1	40.8	5.89	8	1	-6.1	-5.3
2231+3921	3C 449	0.0181	41.0	0.566	2	40.3	4.47	8	1	-5.1	-5.8
2320+0813	NGC 7626	0.0113	<39.8	0.21	1	39.5	>4.85	9	2	<-7.4	-7.6
2338+2701	3C 465	0.0301	41.5	2.12	1	41.3	5.02	8.6	1	-5.3	-5.4

**Table A5. PG Quasars.** References in column 9: [1] Vestergaard (2002), [2] Woo & Urry (2002).

IAU J2000.0	name	$z$	$\log L_B$ [erg/s]	$F_5$ [Jy]	$\log L_R$ [erg/s]	$\log \mathcal{R}$	$\log \mathcal{M}_{BH}$ [ $M_\odot$ ]	ref. to col. 8	$\log L_B$ [ $L_{Edd}$ ]	$\log L_R$ [ $L_{Edd}$ ]
(1)	(2)	(3)	(4)	(5)	(6)	(7)	(8)	(9)	(10)	(11)
0010+1058	PG 0007+106	0.089	44.3	0.321	41.5	2.29	8.3	1	-2.1	-4.9
0029+1316	PG 0026+129	0.142	45.2	0.0051	40.1	0.03	7.6	2	-0.5	-5.6
0053+1241	PG 0050+124	0.061	44.7	0.0026	39.1	-0.48	7.3	1	-0.7	-6.3
0054+2525	PG 0052+251	0.155	45.1	7.4E-4	39.4	-0.62	8.4	2	-1.4	-7.1
0159+0023	PG 0157+001	0.164	45.2	0.008	40.5	0.33	8.0	1	-0.9	-5.7
0810+7602	PG 0804+761	0.1	44.8	0.00238	39.5	-0.22	8.2	2	-1.5	-6.9
0847+3445	PG 0844+349	0.064	44.9	3.1E-4	38.2	-1.56	7.4	2	-0.6	-7.3
0925+1954	PG 0923+201	0.19	45.0	2.5E-4	39.1	-0.84	8.9	2	-2.0	-8.0
0926+1244	PG 0923+129	0.029	43.8	0.01	39.0	0.32	7.0	1	-1.3	-6.1
0956+4115	PG 0953+414	0.239	45.7	0.0019	40.2	-0.36	8.2	2	-0.7	-6.2
1014+0033	PG 1012+008	0.185	45.1	1E-3	39.7	-0.30	8.1	1	-1.1	-6.6
1051-0051	PG 1049-005	0.357	45.7	4.8E-4	40.0	-0.60	9.1	1	-1.6	-7.3
1104+7658	PG 1100+772	0.313	45.6	0.66	43.0	2.51	9.1	1	-1.6	-4.2
1106-0052	PG 1103-006	0.425	45.8	0.482	43.2	2.44	9.3	1	-1.6	-4.2
1117+4413	PG 1114+445	0.144	44.8	2.2E-4	38.8	-0.89	8.4	1	-1.7	-7.7
1119+2119	PG 1116+215	0.177	45.3	0.0028	40.1	-0.14	8.5	1	-1.3	-6.5
1121+1144	PG 1119+120	0.049	44.4	9.4E-4	38.4	-0.82	7.2	1	-0.9	-6.9
1204+2754	PG 1202+28	0.165	45.3	8.3E-4	39.5	-0.73	8.1	1	-0.9	-6.8
1214+1403	PG 1211+143	0.085	44.9	0.157	41.1	1.39	7.5	2	-0.7	-4.5
1219+0638	PG 1216+069	0.334	45.7	0.004	40.8	0.22	9.2	1	-1.6	-6.4
1232+2009	PG 1229+204	0.064	44.6	6.7E-4	38.5	-0.97	8.6	2	-2.1	-8.2
1246+0222	PG 1244+026	0.048	43.8	8.3E-4	38.4	-0.28	6.3	1	-0.6	-6.1
1301+5902	PG 1259+593	0.472	46.0	3E-5	39.1	-1.86	9.0	1	-1.1	-8.0
1309+0819	PG 1307+085	0.155	45.2	3.5E-4	39.0	-1.00	7.9	2	-0.8	-7.0
1312+3515	PG 1309+355	0.184	45.3	0.054	41.4	1.26	8.2	1	-1.1	-4.9
1353+6345	PG 1351+640	0.087	44.6	0.0133	40.1	0.64	8.5	2	-2.0	-6.5
1354+1805	PG 1352+183	0.158	45.0	2.5E-4	38.9	-0.97	8.3	1	-1.4	-7.5
1405+2555	PG 1402+261	0.164	45.1	6.2E-4	39.4	-0.64	7.3	2	-0.3	-6.1
1413+4400	PG 1411+442	0.089	44.8	6.1E-4	38.8	-0.87	7.6	2	-0.9	-6.9
1417+4456	PG 1415+451	0.114	44.7	4E-4	38.8	-0.76	7.8	1	-1.2	-7.1
1419-1310	PG 1416-129	0.129	44.9	0.0036	39.9	0.06	8.5	1	-1.7	-6.7
1429+0117	PG 1426+015	0.086	44.7	0.00121	39.0	-0.55	7.9	2	-1.3	-7.0
1442+3526	PG 1440+356	0.077	44.6	0.00166	39.1	-0.44	7.3	1	-0.8	-6.3
1446+4035	PG 1444+407	0.267	45.4	1.6E-4	39.2	-1.07	8.2	1	-0.9	-7.1
1535+5754	PG 1534+580	0.03	43.6	0.00192	38.3	-0.16	7.4	1	-1.9	-7.2
1547+2052	PG 1545+210	0.266	45.4	0.72	42.9	2.62	9.1	1	-1.9	-4.4
1613+6543	PG 1613+658	0.129	44.9	0.00303	39.8	0	8.6	2	-1.8	-6.9
1620+1724	PG 1617+175	0.114	44.8	0.00109	39.3	-0.38	7.9	2	-1.2	-6.7
1701+5149	PG 1700+518	0.292	45.7	0.0072	41.0	0.37	8.3	2	-0.7	-5.5
2132+1008	PG 2130+099	0.061	44.6	0.00205	39.0	-0.50	7.7	2	-1.3	-6.9
2211+1841	PG 2209+184	0.07	44.2	0.29	41.2	2.15	8.5	1	-2.4	-5.4
2254+1136	PG 2251+113	0.323	45.5	0.523	42.9	2.56	9.0	1	-1.6	-4.1
2311+1008	PG 2308+098	0.432	45.8	0.303	43.0	2.27	9.6	1	-1.9	-4.7